

Brief Articles

Dynamic Combinatorial Mass Spectrometry Leads to Metallo- β -lactamase Inhibitors

Benoît M. R. Liénard,[†] Rebekka Hüting,[†] Patricia Lassaux,[‡] Moreno Galleni,[‡] Jean-Marie Frère,[‡] and Christopher J. Schofield^{*†}

Chemistry Research Laboratory and OCISB, Mansfield Road, Oxford, OX1 3TA, United Kingdom, and Centre d'Ingénierie des Protéines, Université de Liège, Allé du 6 Août B6, Sart-Tilman 4000 Liège, Belgium

Received July 18, 2007

The use of protein ESI mass spectrometry under non-denaturing conditions to analyze a dynamic combinatorial library of thiols/disulfides with the BcII metallo- β -lactamase enabled the rapid identification of an inhibitor with a K_i of $<1 \mu\text{M}$. The study exemplifies the utility of protein-MS for screening dynamic mixtures of potential enzyme-inhibitors.

Introduction

The application of dynamic combinatorial chemistry (DCC)¹ to structure–activity relationship (SAR) studies is limited by the lack of appropriate screening methodology. In some cases, direct protein mass spectrometry provides a potential solution to the problem. Poulsen has recently reported the use of electrospray ionization Fourier transform ion cyclotron resonance (ESI-FTICR) to identify carbonic anhydrase inhibitors from a dynamic combinatorial library (DCL) of hydrazines and aldehydes.² We have applied a combined electrospray ionization mass spectrometry (ESI-MS) and thiol-based DCL approach under non-equilibrating conditions to identify inhibitors of the BcII metallo- β -lactamase (MBL) from *Bacillus cereus*.³ Our Dynamic Combinatorial Mass Spectrometry (DCMS) approach employs a bifunctional dithiol-support ligand in which one thiol is complexed to the active site zinc ions with another thiol-enabling disulfide formation. ESI-MS was used to directly analyze enzyme bound disulfides.

The MBL family are clinically important in resistance to β -lactam antibiotics such as penicillins and carbapenems as they catalyze hydrolysis of almost all the clinically used β -lactam antibiotics.⁴ BcII is a subclass B1 MBL that requires two ZnII ions in its active site for optimal catalytic activity. Among the more potent reported inhibitors for the BcII MBL are the thiols R-thiomandelic acid⁵ and D-captopril.⁶

Here we demonstrate that the DCMS method can be used to identify further disulfides that bind to the BcII MBL and that analogues of these disulfides are potent inhibitors. The demonstration that the approach is not limited to a specific support ligand, coupled to its speed, suggests that the technique may be successfully applied to other targets.

Results and Discussion

Initially, we carried out ESI-MS analyses aimed at identifying support ligands for DCMS screens. We found that mercaptopropionic acid **1** (Figure 1), already known to inhibit the IMP-1 member of the MBL family ($\text{IC}_{50} = 170 \mu\text{M}$),⁷ formed a

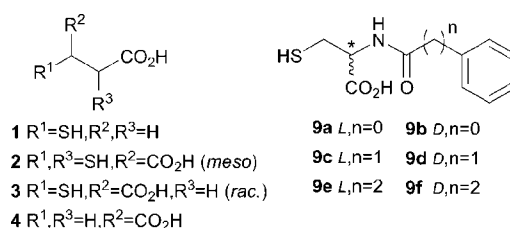


Figure 1. Chemical structures of thiol inhibitors of the BcII MBL.

complex with BcII:Zn_2 that was stable enough to be observed by ESI-MS (Figure 3a).

The commercially available analogue of **1**, *meso*-2,3-dimer-captosuccinic acid (**2**, Figure 1), was then selected for DCMS work, due to its potential ability to interact with BcII:Zn_2 via one SH group and support disulfide exchange using the other thiol (Figures 2 and 3).

The results of the ESI-MS binding assays indicated that **2** binds to BcII:Zn_2 , as shown by a peak corresponding to $\text{BcII:Zn}_2\text{-2}$ (observed $25274 \pm 3 \text{ Da}$; expected 25273 Da ; Figure 3b). Because **3** ($\text{BcII:Zn}_2\text{-3}$; observed $25239 \pm 3 \text{ Da}$; expected 25239 Da ; Figure 3c) but not **4** was observed to bind to BcII:Zn_2 (Figure 3d), and the dizinc site of the BcII:Zn_2 has an affinity for thiol groups,^{8,9} only one thiol group of thiol **2** is likely to chelate by the active site ZnII ions. Together these results indicated that **2** had potential to be used as a support ligand (Figure 2).

The DCMS assay was then applied to a set of thiols (Figure 4) in the presence of BcII. Strikingly, after 30 min of aerial exposure, peaks corresponding to BcII:Zn_2 -disulfide complexes were observed (Figure 3f). Selectivity in the disulfide recognition by the BcII MBL was achieved since, for example, only thiophenols **5a/b/c** and **6a/b/c**, and not carboxybenzylmercaptan **7** (Figure 4), were observed to react with **2** to form disulfide complexes $\text{BcII:Zn}_2\text{-(2}\sim\text{5a/b/c)}$ (observed $25,390 \pm 2 \text{ Da}$; predicted 25390 Da ; Figure 3f; \sim = disulfide bond) and $\text{BcII:Zn}_2\text{-(2}\sim\text{6a/b/c)}$ (observed $25420 \pm 2 \text{ Da}$; predicted 25419 Da ; Figure 3f). This selectivity is different to that observed when using support ligand **8**, which formed a disulfide with **7** and not with **5** or **6** upon binding to BcII:Zn_2 (Figure 3g).³

Because specific disulfides are not necessarily maintained under the condition of the catalytic turnover assays, replacement of the disulfide bond by stable linker analogues was then

* To whom correspondence should be addressed. Tel.: 44 (0) 1865 275 625. Fax: 44 (0) 1865 275 674. E-mail: christopher.schofield@chem.ox.ac.uk.

[†] Chemistry Research Laboratory and OCISB.

[‡] Université de Liège.

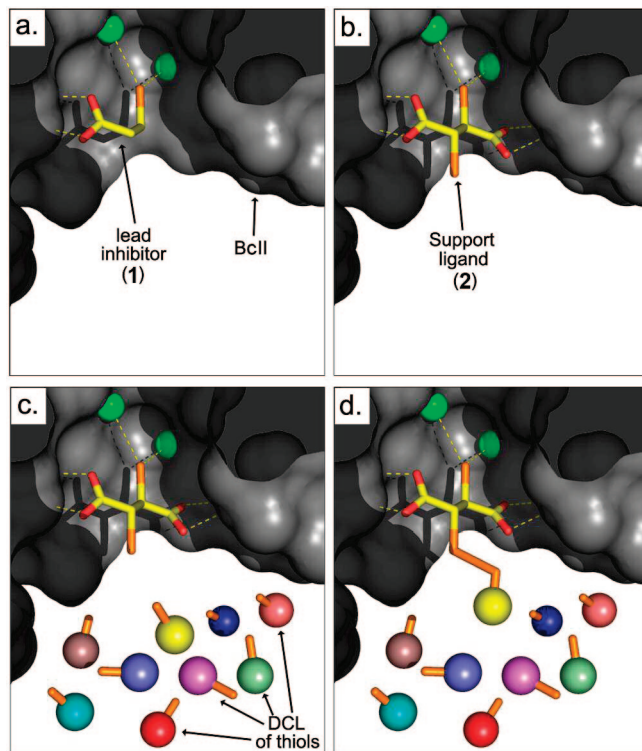


Figure 2. The Dynamic Combinatorial Mass Spectrometry (DCMS) approach. (a) The complex formed by binding of the thiol of the lead compound **1** to the dizinc active site (BcII:Zn₂-**1** complex); (b) The complex formed by binding of the dithiol support ligand **2** with one thiol binding to the dizinc centre leaving one thiol free for disulfide formation (BcII:Zn₂-**2**); (c) The BcII:Zn₂-**2** complex in presence of the dynamic thiol library; (d) Formation of a BcII:Zn₂-disulfide complex; Zn(II) ions are in green, BcII in grey (PDB ID: 1BVT),¹² thiol groups in orange. Figure made using PyMol.

investigated (Figure 3h). ESI-MS studies had indicated that only one of the two carboxylates of **2** was required for binding to BcII:Zn₂ (Figure 3a–d); we thus prepared a series of acylated cysteine-based analogues **9a–f** (Figure 1) as readily prepared analogues of the disulfides observed to bind to BcII:Zn₂. Although imperfect disulfide analogues, the prepared compounds were aimed at imitating the preferred linker length and stereochemistry. Compounds **9a–f** were synthesized in two steps starting from L- and D-cysteine (see Supporting Information) and screened for inhibition versus BcII (Table 1).

The inhibition results revealed that the shortest amido-linker, in agreement with the DCMS data, in combination with a D-cysteine configuration, gave the most potent inhibition, with a K_i value of 740 ± 20 nM for **9b**, consistent with previously reported data on the inhibition of BcII by structurally related compounds.¹⁰ This also represents a significant increase in inhibitory potency (about 170-fold) compared to the lead inhibitor **2**. Inhibition was observed to decrease significantly with increasing linker length coupled to the L-configuration at the cysteine C α , for example, **9c** is 200-fold less potent than **9b**. Furthermore, ESI-MS binding screens of **9a–f** for the binding to BcII:Zn₂ were consistent with the solution inhibition data (see Supporting Information).

The initial DCMS screen had revealed that support ligand **2** selectively forms a disulfide with thiophenols to form BcII:Zn₂ complexes in the presence of aliphatic thiols and benzyl mercaptans. In an attempt to improve the potency of inhibition of **9b** for BcII by optimizing the functionality of its aromatic ring, a further set of thiols comprising exclusively thiophenol derivatives was then employed in a DCMS screen (Figure 5).

Support ligand **2** was incubated with **5**, **6**, and **10** to **17** in the presence of BcII:Zn₂ and the reaction was monitored by ESI-MS. After 24 h of air exposure, three peaks A–C, corresponding to BcII:Zn₂-disulfide complexes with mass shifts of 310, 336, and 343 Da relative to BcII:Zn₂, were observed (Figure 6b). Due to identities or similarities in mass between some of the DCL ligands (e.g., **5** vs **12**), it was not possible to assign the binding partner of **2** using only the mass shifts. Peak A (Figure 6b) could be assigned to either BcII:Zn₂-(**2**~**5a/b/c**) or BcII:Zn₂-(**2**~**12a/b/c**), peak B (Figure 6b) could be assigned to either BcII:Zn₂-(**2**~**6a/b/c**), BcII:Zn₂-(**2**~**13**) or BcII:Zn₂-(**2**~**14**), and peak C (Figure 6b) could be assigned to either BcII:Zn₂-(**2**~**15**) or BcII:Zn₂-(**2**~**17**). Knockout experiments in which specific thiols were deleted were then conducted. The results indicated that upon formation of the mixed disulfide with support ligand **2**, all of **5a–c** (R = NH₂) contributed to a similar extent to the formation of peak A, whereas **12a–c** (R = OH) did not contribute. Peak B was assigned to the BcII:Zn₂-(**2**~**6a/b/c**) (R = CO₂H) and BcII:Zn₂-(**2**~**13**) (R = B(OH)₂) complexes and peak C was assigned to the BcII:Zn₂-(**2**~**15**) (R = NHAc) complex only. It was notable that in the knockout experiments disulfides (**2**~**15**) displayed a significantly stronger binding to BcII:Zn₂ compared to the other disulfides, especially **2**~**17**, which was not observed to bind to BcII:Zn₂.

To test whether the functionalization pattern of the aromatic ring of **9b** obtained in the previous experiments could effectively improve its inhibition against BcII, analogues of disulfides **2**~**15** and **2**~**17** (as a control) were synthesized (see Supporting Information) and tested for inhibition of BcII. Despite remaining relatively potent, BcII inhibitors **18** (Figure 6c, $K_i = 13.5 \pm 0.2$ μ M) and **19** (Figure 6c, $K_i = 8.4 \pm 1$ μ M) did not improve the original inhibitory activity of **9b**. Interestingly, the relative MS binding affinity of **18** for BcII:Zn₂ was significantly stronger than for **19** (see Supporting Information), consistent with the DCMS results, despite having similar K_i values versus BcII.

Conclusions

Overall, our work demonstrates the efficiency of the DCMS technique to rapidly generate inhibitors of clinically relevant enzymes. When this method was used, the inhibitory activity of the lead inhibitor **2** ($K_i = 125$ μ M) versus the BcII MBL was improved by >150-fold, leading to the identification of mercaptocarboxylate **9b** with a K_i value of 740 nM for BcII, 60 times more potent than D-captopril. The work has revealed limitations to the method in that the increased binding affinity, by ESI-MS, of **18** relative to **9b** was not reflected in increased inhibitory potency. This difference may reflect the relative efficiency with which hydrophobic and electrostatic interactions are correlated in solution and under the ESI MS analysis conditions.¹¹ Alternatively, it may reflect the imperfect nature of the disulfide analogues. Another serious limitation is that not all proteins are amenable to nondenaturing MS analyses. However, at least for amenable proteins, the speed with which DCMS data can be generated means the technique is worthy of further investigation.

Experimental Section

DCL Preparation. Individual thiols of the library (**2**, **5**, **6**, and **10–17**) were freshly prepared in DMSO at a final concentration of 100 mM prior to each time-course in a glovebox ($[O_2] < 0.1$ ppm). Each monothiol stock solution (**5**, **6**, and **10–17**) was then diluted to 75 μ M into the same mixture in 15 mM NH₄OAc buffer. The pH of the resulting mixture was then adjusted to pH 7.5 with NH₄OH using a HI 1290 Piccolo pH meter. Support ligand **2** was

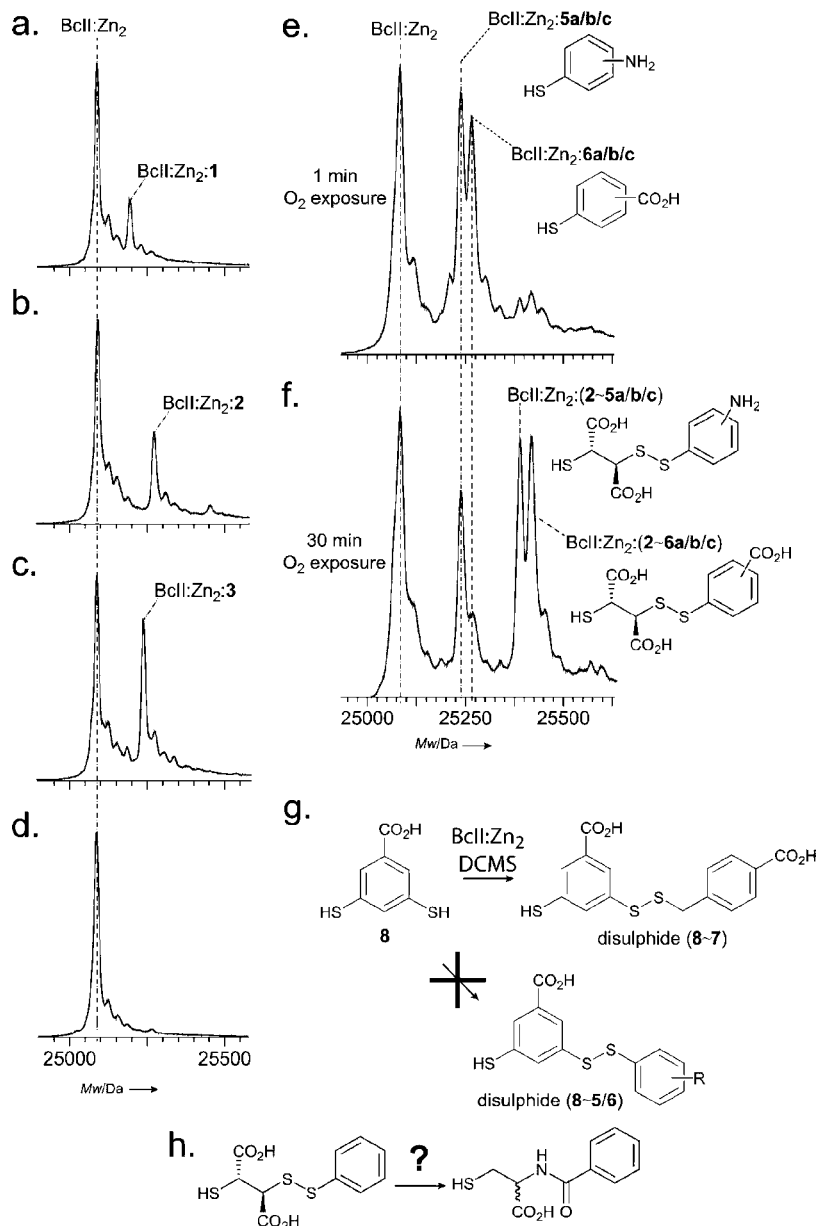


Figure 3. Deconvoluted ESI-MS spectra resulting from BcII:Zn₂ (25089 ± 3 Da) incubated with (a) **1** (106 Da), (b) **2** (182 Da), (c) **3** (150 Da), (d) **4** (118 Da), (e) **2** + DCL of thiol (Figure 4) after 1 min of aerial exposure, (f) **2** + DCL of thiol from Figure 4 after 30 min of aerial exposure, (g) selectivity of the disulfide formation upon binding to BcII:Zn₂ according to the type of support ligand used in the DCMS study (**8** was used as support ligand in previous studies using the set of thiols described in Figure 4);³ and (h) possible structural replacement of the disulfide linkage.

diluted to 100 μM in 15 mM NH₄OAc buffer at pH 7.5. The experimental samples were prepared by mixing the required amounts of the monothiol mixture, **2** and BcII:Zn₂ in NH₄OAc buffer pH 7.5 at a final concentrations of 15, 45, and 15 μM, respectively. A total of 20 μL of this mixture was placed into a 96-well plate sealed with adhesive aluminum foil and taken out of the oxygen-free environment to be analyzed. Samples were kept in ice for the duration of the time-course (except during the time required for measurement).

Soft Ionization Electrospray Mass Spectrometry. ESI-MS analyses used a Q-TOF mass spectrometer (Q-TOFmicro Micro-mass, Altrincham, U.K.) interfaced with a NanoMate chip-based nano-ESI source (Advion Biosciences, Ithaca, NY, U.S.A.). The time-course was started when the nanomate tip pierced the aluminum seal covering the 96-well plate and introduced O₂ into the system. Samples were then infused to the Q-TOF through the ESI chip (estimated flow rate ca. 100 nL/min). Typically a spraying voltage of 1.72 ± 0.1 kV and a sample pressure of 0.25 psi were applied. The instrument was equipped with a standard Z-spray

source block. Clusters of Na_(n+1)I_n (1 mg/mL NaI in 100% methanol) were used for calibration. Calibration and sample acquisitions were performed in the positive ion mode in the range of *m/z* 500–5000. Operating conditions for the mass spectrometer were sample cone voltage (varied) between 50 to 200 V (only the data acquired at sample cone voltage 50 V are shown in the Figures), source temperature 40 °C, and acquisition and scan time were 30 and 1 s, respectively. The pressure at the interface between the atmospheric source and the high vacuum region was fixed at 6.6 mbar (measured with the roughing pump Pirani gauge) by throttling the pumping line using an Edwards Speedivalve to provide collisional cooling.

Kinetic Analyses. Solution of all tested inhibitors were prepared as 10 mM DMSO solutions before dilution with 20 mM HEPES buffer pH 7.0 containing 20 μg/mL BSA. The enzyme and inhibitor were preincubated at room temperature before the substrate (imipenem) was added. Substrate concentrations were varied between 20 and 200 μM at a minimum of two inhibitor concentrations and in its absence. Hydrolysis of imipenem was monitored by following the variation in absorbance at 300 or 482 nm,

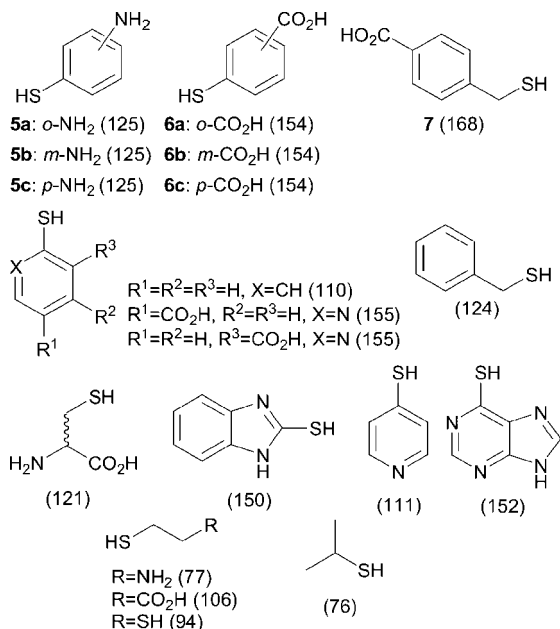


Figure 4. Dynamic thiol library: first set (MW in Da).

Table 1. *K_i* Values vs the BcII MBL

compd	<i>K_i</i> (μM)	compd	<i>K_i</i> (μM)
2	125 ± 11	9d	53 ± 1
9a	28 ± 0.5	9e	44 ± 1.5
9b	0.74 ± 0.02	9f	73 ± 1
9c	154 ± 5		

respectively, using a Uvikon 860 spectrophotometer connected to a computer via a RS232 serial interface. Cells of 2 or 10 mm path length were used depending on substrate concentration. The experiments were performed at 30 °C and initial rate conditions were used to study the inhibition with imipenem using the Hanes linearization of the Henri–Michaelis equation and the KaleidaGraph 3.5 program.

***N*-Benzoyl-L-cysteine (9a).** Compound **9a** was prepared following a reported method.¹⁰ IR ν_{\max} (film) 3014 (b, OH), 2552 (m, SH), 1732 (s, C=O), 1639 (s, C=O), 1216 (s, C–O) cm⁻¹; ¹H NMR (500 MHz, DMSO-*d*₆) δ 12.85 (brs, 1H, COOH), 8.65 (d, *J* = 8.0 Hz, 1H, NH), 7.91–7.90 (m, 2H, ArH), 7.59–7.55 (m, 1H, ArH), 7.51–7.49 (m, 2H, ArH), 4.55–4.51 (m, 1H, H_α), 3.03–3.01 (m, 1H, H_β), 2.92–2.88 (m, 1H, H_β), 2.60 (brs, 1H, SH); ¹³C NMR (126 MHz, DMSO-*d*₆) δ 172.3 (C=O), 167.0 (C=O), 134.3 (ArC), 132.0 (ArCH), 128.8 (2 × ArCH), 127.9 (2 × ArCH), 56.0 (CH_α), 25.7 (CH₂); HRMS (ESI⁻) (*M* – H)⁻ calcd for C₁₀H₁₀NO₃S⁻, 224.0381; found, 224.0676; [α]_D²⁵ = –15° (*c* = 0.54, CH₃OH).

***N*-Benzoyl-D-cysteine (9b).** Compound **9b** was prepared following a reported method.¹⁰ All analytical data were identical to that of **9a**, with the exception of the optical rotation: [α]_D²⁵ = +19° (*c* = 0.48, CH₃OH).

***N*-Phenylacetyl-L-cysteine (9c).** Compound **9c** was prepared following a reported method.¹⁰ Mp 96–98 °C; ¹H NMR (400 MHz,

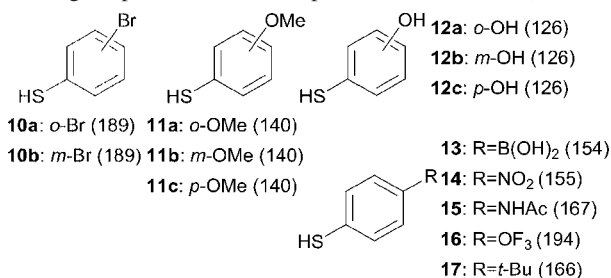


Figure 5. Dynamic thiol library: second set (MW in Da).

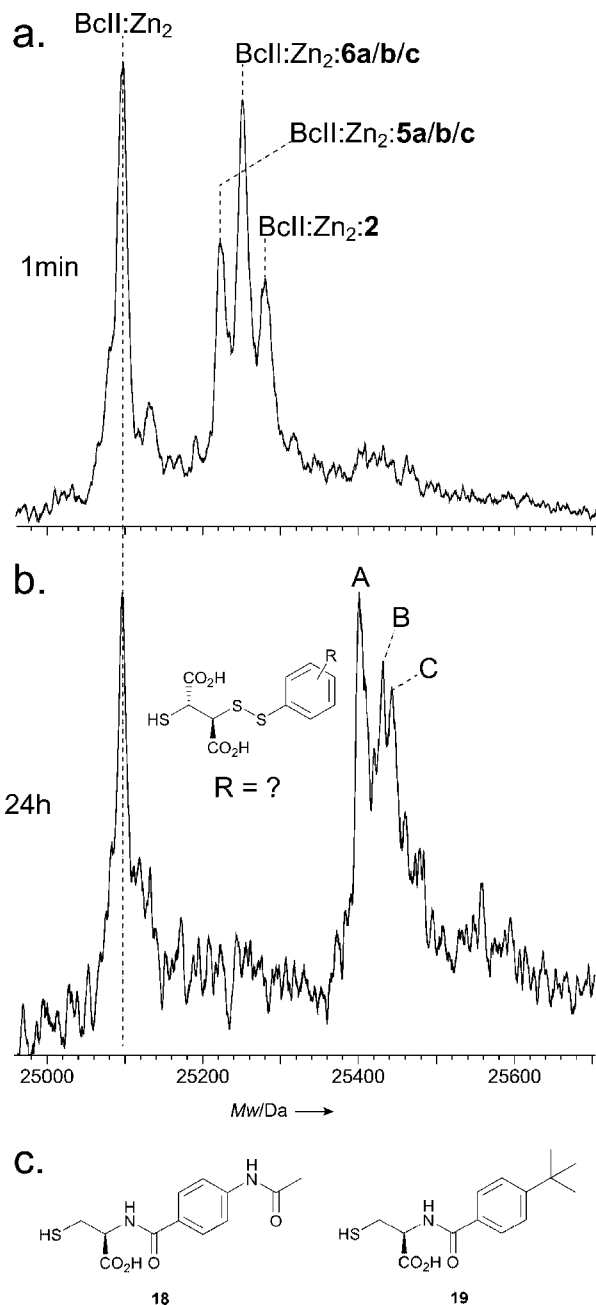


Figure 6. Deconvoluted ESI-MS spectra resulting from BcII:Zn₂ incubated with support ligand **2** and the DCL of thiols (Figure 4) after (a) 1 min and (b) 24 h of aerial exposure. Peaks A, B, and C correspond to BcII:Zn₂–disulfide quaternary complexes with a mass shift related to BcII:Zn₂ of 310, 336, and 343 Da, respectively; (c) derivatives of **9b** designed according to the results of the second DCMS study (b).

DMSO-*d*₆) δ 12.90 (s, 1H), 8.43 (d, *J* = 8.0 Hz, 1H), 7.33–7.19 (m, 5H), 4.40 (ddd, *J* = 8.0 Hz, *J* = 8.0 Hz, *J* = 5.0 Hz, 1H), 3.52 (s, 2H), 2.87 (ddd, *J* = 13.5 Hz, *J* = 8.5 Hz, *J* = 5.0 Hz, 1H), 2.80–2.73 (m, 1H), 2.39 (t, *J* = 8.5 Hz, 1H); ¹³C NMR (126 MHz, DMSO-*d*₆) δ 172.5, 171.1, 137.0, 129.9 (× 2), 129.0 (× 2), 127.2, 55.3, 42.8, 26.5; HRMS (ESI⁻) (*M* – H)⁻ calcd for C₁₁H₁₂NO₃S⁻, 238.0538; found, 238.0532; [α]_D²⁵ = +2.8° (*c* = 0.5, CH₃OH).

***N*-Phenylacetyl-D-cysteine (9d).** Compound **9d** was prepared following a reported method.¹⁰ All analytical data were identical to that of **9c**, with the exception of the optical rotation: [α]_D²⁵ = –1.6° (*c* = 0.24, CH₃OH).

***N*-Phenylpropionyl-L-cysteine (9e).** Compound **9e** was prepared following a reported method.¹⁰ Mp 126–127 °C (white crystalline solid); IR ν_{\max} (KBr disk) 3353 (s, OH), 1721 (s, C=O), 1617 (s, C=O), 1224 (s, C–O) cm⁻¹; ¹H NMR (400 MHz, DMSO-*d*₆) δ

12.83 (brs, 1H, COOH), 8.20 (d, $J = 8.0$ Hz, 1H, NH), 7.29–7.15 (m, 5H, ArH), 4.40 (ddd, $J = 8.0$ Hz, $J = 7.5$ Hz, $J = 4.5$ Hz, 1H, H_{α}), 2.84–2.80 (m, 3H, $CH_2 + H_{\beta}$), 2.75–2.66 (m, 1H, H_{β}), 2.52–2.41 (m, 2H, CH_2), 2.29 (brs, 1H, SH); ^{13}C NMR (101 MHz, DMSO- d_6) δ 172.6 (C=O), 172.4 (C=O), 142.1 (ArC), 129.14 (2 \times ArCH), 129.12 (2 \times ArCH), 126.8 (ArCH), 55.2 (CH_{α}), 37.5 (CH_2), 31.9 (CH_2), 26.5 ($CH_2\beta$); HRMS (ESI $^+$) (M + Na) $^+$ calcd for $C_{12}H_{15}NNaO_3S^+$, 276.0670; found, 276.0665; $[\alpha]^{25}_D = -6^\circ$ ($c = 0.62$, CH_3OH).

N-Phenylpropionyl-D-cysteine (9f). Compound **9f** was prepared following a reported method.¹⁰ All analytical data were identical to that of **9e** with the exception of the optical rotation: $[\alpha]^{25}_D = +6.4^\circ$ ($c = 0.32$, CH_3OH).

N,N'-Bis(4-Acetamidobenzoyl)-D-cysteine (18). Compound **18** was prepared following a reported method.¹⁰ Mp 205–210 °C (white solid); IR ν_{max} (KBr disk) 3342 (s, OH), 2550 (m, SH), 1716 (s, C=O), 1640 (s, C=O), 1593 (s, C=O); 1H NMR (500 MHz, DMSO- d_6) δ 12.84 (s, 1H, COOH), 10.17 (s, 1H, NH), 8.49 (d, $J = 8.5$ Hz, 1H, NH), 7.84 (d, $J = 8.5$ Hz, 2H, ArH), 7.66 (d, $J = 8.5$ Hz, 2H, ArH), 4.49 (ddd, $J = 9.0$ Hz, $J = 8.0$ Hz, $J = 4.5$ Hz, 1H, H_{α}), 2.96–3.01 (m, 1H, H_{β}), 2.84–2.90 (m, 1H, H_{β}), 2.56 (t, $J = 8.5$ Hz, 1H, SH), 2.07 (s, 3H, CH_3); ^{13}C NMR (126 MHz, DMSO- d_6) δ 171.9 (C=O), 168.7 (C=O), 166.0 (C=O), 142.2 (ArC), 128.4 (2 \times ArCH), 128.0 (ArC), 118.0 (2 \times ArCH), 55.5 (CH_{α}), 25.2 ($CH_2\beta$), 24.1 (CH_3); HRMS (ESI $^+$) (M + Na) $^+$ calcd for $C_{12}H_{14}N_2NaO_4S_1^+$, 305.0572; found, 305.0566; $[\alpha]^{25}_D = +23^\circ$ ($c = 0.08$, CH_3OH).

N-(4-tert-Butylbenzoyl)-D-cysteine (19). Compound **19** was prepared following a reported method.¹⁰ Mp 115–118 °C (white crystalline solid); IR ν_{max} (KBr disk) 3345 (b, OH), 2569 (m, SH), 1733 (s, C=O), 1638 (s, C=O) cm^{-1} ; 1H NMR (500 MHz, DMSO- d_6) δ 8.52 (d, $J = 8.5$ Hz, 1H, NH), 7.82 (d, $J = 8.5$ Hz, 2H, ArH), 7.50 (d, $J = 8.5$ Hz, 2H, ArH), 4.49 (ddd, $J = 9.0$ Hz, $J = 8.5$ Hz, $J = 4.5$ Hz, 1H, H_{α}), 2.99 ($J = 13.5$ Hz, $J = 9.0$ Hz, 1H, H_{β}), 2.88 ($J = 13.5$ Hz, $J = 9.0$ Hz, 1H, H_{β}), 1.31 (s, 9H, t -Bu); ^{13}C NMR (126 MHz, DMSO- d_6) δ 172.3 (COOH), 166.4 (CONH), 144.3 (ArC), 131.1 (ArC), 127.3 (2 \times ArCH), 125.1 (2 \times ArCH), 55.4 (CH_{α}), 34.6 (C - t -Bu), 31.0 (3 \times t -Bu), 25.3 ($CH_2\beta$); HRMS (ESI $^+$) (M + Na) $^+$ calcd for $C_{14}H_{19}NNaO_3S_1^+$, 304.0978; found, 304.0978; $[\alpha]^{25}_D = +23.3^\circ$ ($c = 0.42$, CH_3OH).

Acknowledgment. We thank the Biotechnology and Biological Sciences Research Council and the E.U. (Contract No. HPRN-CT-2002-00264) for support of B.M.R.L. and P.L.

Supporting Information Available: Experimental details corresponding to the synthesis of the compounds described in this paper

and additional ESI-MS experiments. This material is available free of charge via the Internet at <http://pubs.acs.org>.

References

- (1) Corbett, P. T.; Leclaire, J.; Vial, L.; West, K. R.; Wietor, J. L.; Sanders, J. K.; Otto, S. Dynamic combinatorial chemistry. *Chem. Rev.* **2006**, *106* (9), 3652–711.
- (2) Poulsen, S. A.; Bornaghi, L. F. Fragment-based drug discovery of carbonic anhydrase II inhibitors by dynamic combinatorial chemistry utilizing alkene cross metathesis. *Bioorg. Med. Chem.* **2006**, *14* (10), 3275–84.
- (3) Liénard, B. M.; Selevsek, N.; Oldham, N. J.; Schofield, C. J. Combined mass spectrometry and dynamic chemistry approach to identify metalloenzyme inhibitors. *ChemMedChem* **2007**, *2* (2), 175–9.
- (4) Bush, K.; Jacoby, G. A.; Medeiros, A. A. A functional classification scheme for beta-lactamases and its correlation with molecular structure. *Antimicrob. Agents Chemother.* **1995**, *39* (6), 1211–33.
- (5) Mollard, C.; Moali, C.; Papamicael, C.; Damblon, C.; Vessilier, S.; Amicosante, G.; Schofield, C. J.; Galleni, M.; Frere, J. M.; Roberts, G. C. Thiomandelic acid, a broad spectrum inhibitor of zinc beta-lactamases: Kinetic and spectroscopic studies. *J. Biol. Chem.* **2001**, *276* (48), 45015–23.
- (6) Heinz, U.; Bauer, R.; Wommer, S.; Meyer-Klaucke, W.; Papamichaels, C.; Bateson, J.; Adolph, H. W. Coordination geometries of metal ions in D- or L-captopril-inhibited metallo-beta-lactamases. *J. Biol. Chem.* **2003**, *278* (23), 20659–66.
- (7) Siemann, S.; Clarke, A. J.; Viswanatha, T.; Dmitrienko, G. I. Thiols as classical and slow-binding inhibitors of IMP-1 and other binuclear metallo-beta-lactamases. *Biochemistry* **2003**, *42* (6), 1673–83.
- (8) Concha, N. O.; Janson, C. A.; Rowling, P.; Pearson, S.; Cheever, C. A.; Clarke, B. P.; Lewis, C.; Galleni, M.; Frere, J. M.; Payne, D. J.; Bateson, J. H.; Abdel-Meguid, S. S. Crystal structure of the IMP-1 metallo beta-lactamase from *Pseudomonas aeruginosa* and its complex with a mercaptocarboxylate inhibitor: binding determinants of a potent, broad-spectrum inhibitor. *Biochemistry* **2000**, *39* (15), 4288–98.
- (9) Damblon, C.; Jensen, M.; Ababou, A.; Barsukov, I.; Papamicael, C.; Schofield, C. J.; Olsen, L.; Bauer, R.; Roberts, G. C. The inhibitor thiomandelic acid binds to both metal ions in metallo-beta-lactamase and induces positive cooperativity in metal binding. *J. Biol. Chem.* **2003**, *278* (31), 29240–51.
- (10) Bounaga, S.; Galleni, M.; Laws, A. P.; Page, M. I. Cysteinylyl peptide inhibitors of *Bacillus cereus* zinc beta-lactamase. *Bioorg. Med. Chem.* **2001**, *9* (2), 503–10.
- (11) Gao, J.; Cheng, X.; Chen, R.; Sigal, G. B.; Bruce, J. E.; Schwartz, B. L.; Hofstadler, S. A.; Anderson, G. A.; Smith, R. D.; Whitesides, G. M. Screening derivatized peptide libraries for tight binding inhibitors to carbonic anhydrase II by electrospray ionization-mass spectrometry. *J. Med. Chem.* **1996**, *39*, 1949–1955.
- (12) Carfi, A.; Duee, E.; Galleni, M.; Frere, J. M.; Dideberg, O. 1.85 Å resolution structure of the zinc (II) beta-lactamase from *Bacillus cereus*. *Acta Crystallogr., Sect. D: Biol. Crystallogr.* **1998**, *54* (Pt 3), 313–23.

JM070866G